

A DETERMINATION OF INTERFACE FREE ENERGIES

Alain Billoire

Service de Physique Théorique de Saclay*
91191 Gif-sur-Yvette Cedex, France

Thomas Neuhaus

Fakultät für Physik, Universität Bielefeld
D-W 4800 Bielefeld, FRG

and Bernd A. Berg[†]

Wissenschaftskolleg zu Berlin
Wallotstraße 19, D-W 1000 Berlin 33, FRG

July 26 1993

We determine the interface free energy $F_{o.d.}$ between disordered and ordered phases in the $q=10$ and $q=20$ 2-d Potts models using the results of multicanonical Monte Carlo simulations on L^2 lattices, and suitable finite volume estimators. Our results, when extrapolated to the infinite volume limit, agree to high precision with recent analytical calculations. At the transition point β_t the probability distribution function of the energy exhibits two maxima. Their locations have $1/L^2$ corrections, in contradiction with claims of $1/L$ behavior made in the literature. Our data show a flat region inbetween the two maxima which characterizes two domain configurations.

SPhT-93/065

*Laboratoire de la Direction des Sciences de la Matière du CEA.

[†]On sabbatical from the Florida State University.

1 Introduction

First order phase transitions play an important role in statistical mechanics as well as in field theory, see for instance [1]. For example, the finite temperature phase transition of Quantum Chromo Dynamics and the symmetry restoration phase transition of the weak interaction theory are likely to be first order. The value of the interface free energy is a parameter of great importance. It determines the non-equilibrium properties of the phase transition. In this paper we address the question of how to determine the value of the interface free energy using Monte Carlo simulations. For this purpose we consider much simpler models namely the 2-d $q=10$ and $q=20$ Potts models [2], which in statistical mechanics are prototype models of systems with first order phase transitions.

Recently two interesting analytical results have been obtained for Potts models in the first order phase transition region. One is a rigorous theory of finite size scaling (FSS) [3, 4], which has been proven for large values of q , although it is likely to hold for all $q > 4$. However, it has been found numerically that very large lattices are required in order to observe the predicted behavior [5]. The other result are calculations of the 2-d spin-spin correlation length at the infinite volume phase transition point β_t [6, 7]. The exact value of the order-disorder interface free energy $F_{o.d.}$ follows [8]. These results could then be compared with previously obtained Monte Carlo (MC) results, of which the multicanonical [9, 10] proved to be most accurate. Table 1 displays the exact interface free energy for $q=7, 10$ and 20 together with MC estimates. Although the overall accuracy of the MC estimates is quite satisfactory, it seems that there are uncontrolled systematic errors larger than the estimated statistical error. It is thus a challenge to improve the methods employed for infinite volume estimates from finite volume numerical calculations. These questions are addressed in the next two sections of the paper. In section 4 we analyze multicanonical MC data for $q=10$ and 20 . Section 5 summarizes the final conclusions.

2 Finite Volume Energy Distribution

We consider L^d lattices with periodic boundary conditions. In the 2-d Potts model the energy density ranges in steps of $1/L^2$ in the interval $-2 \leq E \leq 0$. Numerical simulations yield statistical estimates of the canonical probability density $P_L(\beta, E)$. In this paper we are concerned with the shape of $P_L(\beta, E)$ in the vicinity of the transition point β_t , in order to extract the interface free energy $F_{o.d.}$. In the transition region one expects for $P_L(\beta, E)$ the existence of two distinct maxima $P_L^{max,o}$ and $P_L^{max,d}$, corresponding to the ordered and disordered bulk states of the system. These are centred at separated values of the energy $E_L^{max,o}$ and $E_L^{max,d}$. Inbetween there will be a value of the energy

E_L^{min} where $P_L(\beta, E)$ takes its minimal value P_L^{min} . States with energies close to E_L^{min} correspond to configurations containing two interfaces.

Following [3], we can write the partition function for the q -state Potts model on a L^d lattice with periodic boundary conditions in the form

$$Z_L(\beta) = e^{-L^d \beta f_d(\beta)} + q e^{-L^d \beta f_o(\beta)} + \mathcal{O}(e^{-bL}) e^{-\beta f(\beta) L^d} \quad ; \quad b > 0. \quad (1)$$

Here are $f_o(\beta)$ and $f_d(\beta)$ smooth L independent functions, representing the free energy densities of the ordered and disordered phases. Furthermore one has $f(\beta) = \min\{f_o(\beta), f_d(\beta)\}$. At β_t both free energies become equal to $f(\beta_t)$. In the vicinity of β_t they possess the expansions

$$\beta f_i(\beta) = \beta f(\beta_t) + (\beta - \beta_t) E_i + \frac{(\beta - \beta_t)^2}{2} \left(\frac{-C_i}{\beta_t^2} \right) + \dots \quad (2)$$

with $i = o, d$ respectively. The C_i and the E_i denote infinite volume specific heat and energy densities at β_t . In 2-d they have the exact values [11] $E_o = -1.66425$, $E_d = -0.96820$, $C_d - C_o = 0.44763$ for $q=10$ and $E_o = -1.82068$, $E_d = -0.62653$, $C_d - C_o = 0.77139$ for $q=20$. The large q expansion of [12] gives $C_o = 18.06(4)$ and $C_o = 5.362(3)$, in addition numerical simulations indicate $C_o = 12 - 18$ for $q=10$ and $C_o = 5.2(2)$ for $q=20$ [13, 5].

We obtain the density of states $\Omega_L(E)$ by inverse Laplace transform.

$$\Omega_L(E) = \frac{L^d}{2\pi i} \int_{c-i\infty}^{c+i\infty} e^{L^d \zeta E} Z_L(\zeta) d\zeta. \quad (3)$$

We now consider the specific form $Z_L(\beta) = \exp(-L^d g(\beta))$, which is the form of the partition function of each of the bulk phases of eq.(1), neglecting terms $\mathcal{O}(e^{-bL})$ (we understand that this is not a valid procedure for values of E close to E_L^{min} , see below). It follows

$$\Omega_L(E) = \frac{L^d}{2\pi i} \int_{c-i\infty}^{c+i\infty} e^{L^d(\zeta E - g(\zeta))} d\zeta. \quad (4)$$

This integral is computed using the steepest descent method. The saddle point is at $\zeta = \beta_s(E)$ which is solution of the equation

$$E = \left. \frac{\partial g(\zeta)}{\partial \zeta} \right|_{\zeta=\beta_s(E)}. \quad (5)$$

$\beta_s(E)$ is the value of β for which E is the internal energy of the system. Since

$$\left. \frac{\partial^2 g(\zeta)}{\partial^2 \zeta} \right|_{\zeta=\beta_s(E)} = -T^2 C(\beta_s(E)) \quad (6)$$

is negative the straight path $\zeta = \beta_s + ix$, with x real, is the steepest descent, and we obtain the saddle point approximation

$$\Omega_L(E) \approx \frac{L^{d/2} e^{L^d (E\beta_s(E) - g(\beta_s(E)))}}{\sqrt{-2\pi \frac{\partial^2 g(\zeta)}{\partial \zeta^2} \Big|_{\zeta=\beta_s(E)}}}. \quad (7)$$

The gaussian approximation for $P_L(\beta, E) = \frac{1}{Z_L(\beta)} e^{-\beta EL^d} \Omega_L(E)$ is obtained expanding E around $\bar{E}_i(\beta)$, the internal energy at β , then

$$P_L(\beta, E) \approx \sum_{i=d,o} (\delta_{d,i} + q\delta_{o,i}) \sqrt{\frac{L^d}{2\pi T^2 C_i(\beta)}} e^{-\frac{(E - \bar{E}_i(\beta))^2 L^d}{2T^2 C_i(\beta)}} e^{-\beta f_i(\beta) L^d}. \quad (8)$$

This form corresponds to Binder's ansatz for $P_L(\beta, E)$ in the vicinity of a first order transition point [14]. In this approximation the locations of the maxima $E_L^{max,i}$ of $P_L(\beta, E)$ show no finite volume dependence. In order to find the dependence, one keeps one more term in the expansion of $g(\beta)$. Then $g''|_{\zeta=\beta_s(E)} \approx g''|_{\zeta=\beta} + (E - \bar{E}(\beta)) g'''|_{\zeta=\beta}/g''|_{\zeta=\beta}$, $E_L^{max,i} \approx \bar{E}_i + (g'''/(2g''L^d))$. This effect is due the asymmetry of the fluctuations inside each bulk phase, and is not the one advocated in [15].

A few remarks on the two Gaussian approximation are appropriate here.

- The two Gaussian approximation predicts at the transition point β_t a ratio $R_q = P_L^{max,o}/P_L^{max,d} = q\sqrt{C_d/C_o}$. Putting in actual numbers for C_o and C_d we find $R_{10} = 10.12$ for $q=10$ and $R_{20} = 21.4$ for $q=20$. The ratio of the weights of the ordered and disordered states is precisely equal to q . This follows from eq.(1) and does not rely on the gaussian approximation.

- The widths of the two peaks of $P_L(\beta, E)$ are predicted, namely

$$\sigma_i = \frac{1}{L^{\frac{d}{2}} \beta_t} \sqrt{2C_i}. \quad (9)$$

- Inbetween the two maxima the Gaussian approximation is incorrect. In this region mixed phase configurations dominate, this is the subject of the next section.

3 Mixed Phase Configurations

For energies between the two peaks and large L , the probability to be in a pure phase is suppressed like $\exp[-(E - \bar{E})^2 L^d / (2T^2 C_i)]$. Mixed phase configurations, where each phase occupies a macroscopic fraction of the system, become dominant [16] since they are only suppressed like $\exp(-\sigma_{o,d} \cdot \text{const} \cdot L^{d-1})$,

where $\sigma_{o,d}$ is the order disorder interface tension and $\text{const.}L^{d-1}$ the interface area (interface length for 2-d). Sufficiently close to E_L^{min} the configurations with minimum interface area contains two planar interfaces, closed by periodic boundary conditions. Closer to the peaks configurations with minimum interface are made of a single macroscopic bubble of one phase inside the other phase. The shape of the bubble is given by the Wulff construction, it is spherical when the correlation length becomes infinite. The interface area of a two planar interface configuration is $2L^{d-1}$. In the 2-d case, it dominates over the spherical bubble configuration for

$$E^- < E < E^+ \quad (10)$$

with

$$E^- = E_o - \frac{1}{\pi}(E_o - E_d), \quad (11)$$

$$E^+ = E_d + \frac{1}{\pi}(E_o - E_d). \quad (12)$$

Such a behavior has been rigourously shown to occur for the order order magnetic transitions of the 2-d Ising model in the broken phase [17]. Numerically it was observed for the 2-d and 3-d Ising models [18]. Two planar interface configurations, with a fraction x of the volume in the ordered phase, contribute to the partition function as

$$Z^{\text{mixed}}(x) \propto e^{-xL^d\beta f_o(\beta)} \times e^{-(1-x)L^d\beta f_d(\beta)} \times L^p e^{-F_{o,d}L^{d-1}}. \quad (13)$$

The first two factors are contributions from the pure phases. The factor $L^p \exp(-F_{o,d}L^{d-1})$ comes from interface effects, $F_{o,d} = 2\sigma_{o,d}$ and $p = d - 1$ in the capillary wave approximation [19, 20].

At the infinite volume transition point β_t the free energy densities f_o and f_d equal $f(\beta_t)$. $Z^{\text{mixed}}(x)$ will then asymptotically have the x -independent form

$$Z^{\text{mixed}}|_{\beta=\beta_t} \propto e^{-L^d\beta_t f(\beta_t)} \times L^p e^{-F_{o,d}L^{d-1}}. \quad (14)$$

It means that in the region around E_L^{min} the probability distribution $P_L(\beta_t, E) = Z^{\text{mixed}}/Z \propto L^p \exp(-F_{o,d}L^{d-1})$ is flat. This formula could be used to determine the interface tension. However, we found it more convenient to use the ratio $\sqrt{P_L^{\text{max},o} P_L^{\text{max},d}}/P_L^{\text{min}} \propto L^{-p+d/2} \exp(F_{o,d}L^{d-1})$, and introduce the finite volume estimator

$$F(L) = \frac{1}{2L^{d-1}} \ln\left[\frac{P_L^{\text{max},o} P_L^{\text{max},d}}{(P_L^{\text{min}})^2}\right] |_{\beta=\beta_t} \quad (15)$$

$$= F_{o,d} + \frac{a_1}{L^{d-1}} + \left(-p + \frac{d}{2}\right) \frac{\ln(L)}{L^{d-1}} + \frac{a_2}{L^d} + \frac{a_3}{L^{d+1}} + \dots \quad (16)$$

It is convenient to consider $P_L(\beta_t, E)$ because one can check whether it has a flat part as it should. If it does not, the value of $F_{o,d}$ extracted from eq. (16) is questionable. However this equation, with $L^d(\beta - \beta_t)$ dependent a_i 's, holds asymptotically for all β in a $\propto 1/L^d$ neighborhood of β_t (e.g. at the equal heights point like in [9]).

4 Numerical Results

The simulations have been performed with the multicanonical algorithm [9], for more information we refer to [5]. For $q=10$ we have simulated lattices in the range from 12^2 to 100^2 , for $q=20$ from 16^2 to 70^2 . The statistics for $q=10$ is given in [9], for $q=20$ in [5], and additional $q=20$ statistics is collected in Table 2. Errors quoted in this paper are bias corrected jackknife estimates. The simulations have been performed on the Saclay Cray X-MP, on RISC stations of the SCRI workstation cluster and on an ALPHA station at Bielefeld University.

For the determination of the quantities $P_L^{max,o}$, $P_L^{max,d}$, $E_L^{max,o}$ and $E_L^{max,d}$ we adopt the following procedure. After locating approximate values we fit the probability function $P_L(\beta_t, E)$ in the vicinity of the maxima on an energy interval corresponding to a decrease of $P_L(\beta_t, E)$ by at most a factor $1/e$ of its maximal value. We use the cubic form

$$\ln P_L(\beta_t, E) = \text{const} + \frac{(E - E_L^{max,i})^2}{\sigma_i} + \alpha(E - E_L^{max,i})^3. \quad (17)$$

We have checked that the fits gave acceptable $\chi^2/d.o.f$ values. Figure 1 displays an example for the $q=20$ model on a 50^2 lattice. It can be seen that the probability distribution in vicinity of the maximum shows a sizable asymmetry, demonstrating that the cubic term is needed in order to give a good description of the data. For the determination of the quantities P_L^{min} and E_L^{min} we found it sufficient to use a quadratic fit analogue to eq.(17) with $\alpha = 0$. An example of such a fit is displayed in Figure 2.

Using eq.(9) and the width parameters σ_i for $i = o, d$ as obtained by the fit (17) we determine finite volume estimators of the specific heats $C_o(L)$ and $C_d(L)$. The results are collected in Table 3 for $q=10$ and in Table 4 for $q=20$. Figure 3 displays a plot of $C_o(L)$ for $q=10$ and $q=20$, together with asymptotic values predicted by a large q -expansion [12]. In case of $q=20$ our data for $C_o(L)$ converge towards a value consistent with the large q expansion results and the FSS study [5] that gives $C_o = 5.2(2)$. In addition, the data for $C_d(L) - C_o(L)$ approach, as L grows, the exactly known infinite volume limit. For the $q=10$ model the data overshoot the value $C_o = 12.7(3)$, obtained from the FSS of the extrema of the specific heat [13]. The value indicated by the large q -expansions is $C_o = 18.06(4)$. A value $C_o \approx 18$ was

obtained in [13] from the FSS of the specific heat at β_t . Much larger lattices would be required in order to see $C_o(L)$ approach this limit (The correlation length [7] at β_t is $\xi_{disorder} = 10.56$ for $q = 10$ and 2.70 for $q = 20$).

In figure 4 to 7 we display the locations of the maxima $E_L^{max,o}$ and $E_L^{max,d}$ of the energy probability distribution function at β_t as function of the variable $1/L^d$, compared with the prediction $E_L^{max,i} = \bar{E}_i + const./L^d$ with slopes [12] 100 ($q = 10$) and 15 ($q = 20$). The data are collected also in Tables 3 and 4. For our largest lattices the predicted linear dependence on $1/L^d$ is born out. The deviations observed can be reproduced [21] within the formalism of [12]. This rules out the $1/L$ behavior predicted in [15]. For the larger sized lattices the ratio R_q become consistent with the theoretical prediction $q\sqrt{C_d/C_o}$. These tables contain also our estimates for the partition functions ratios $Z_L^o(\beta_t)/Z_L^d(\beta_t)$. They are defined by summing the probability distribution function at β_t over corresponding energy ranges $E < E_L^{min}$, resp. $E > E_L^{min}$. These ratios are consistent with the value q as predicted by theory. Unfortunately, due to small numbers of tunneling events, they have sizable errors on our largest lattices.

In figure 8 we display a selection of our data for the probability distribution function $P_L(\beta_t, E)$ for the $q=20$ Potts model. An analogous figure for the $q=10$ Potts model can be found in [9]. We observe the unfolding of a flat region of the probability distribution function on our largest lattices $L > 38$, therefore giving direct numerical evidence for the dominance of two planar interface configurations. On the 50^2 , 60^2 and 70^2 lattices we have tried to estimate the limits of the energy range where this occurs. For this purpose we have numerically estimated the curvature of the probability distribution function. We assume that on finite lattices the locations of largest curvature determine the limits. An example of this procedure is displayed in figure 9. The obtained values, as collected in Table 5, are rather close to the values E^\pm of the spherical bubble model.

Tables 3 and 4 also contain our results for the finite volume estimators of the interface free energy $F(L)$. They have been plotted in figures 10 and 11 as a function of the variable $1/L$. The horizontal line in these figures always denotes the known analytical value [7]. It can be seen that in case of the $q=10$ model the finite size behavior of $F(L)$ is very well described, in the whole L range, by a correction proportional to $1/L$ (*i.e.* $p = 1$) as predicted by the capillary wave approximation. However in the $q=20$ Potts model we find a more complicated behavior. We cannot draw a conclusion on the actual form of the functions $F(L)$, *i.e.* it is undecided whether logarithmic corrections are present or not.

We have performed several fits with the form eq.(16). We have successively freed higher order corrections in $1/L$ and also varied the interval of lattices sizes. The results of this fits together with their $\chi^2/d.o.f.$ values are collected in Tables 6 and 7. All fits of Table 6 and most fits of Table 7 are

within one standard deviation consistent with the exact $F_{o.d.}$ result of table 1 (In the $q = 10$ case, this consistency is obtained although we do not observe the expected flat part in $P_L(\beta_t, E)$, in the $q = 20$ case this consistency requires either to omit small lattice data, or to include $1/L^2$ corrections).

As our final result we quote

$$F_{o.d.} = 0.0950(5) \text{ for } q = 10 \quad (18)$$

and

$$F_{o.d.} = 0.3714(13) \text{ for } q = 20. \quad (19)$$

5 Conclusion

We have presented a careful analysis of properties of the probability distribution function $P_L(\beta, E)$ in the 2-d $q=10$ and $q=20$ Potts model at the infinite volume transition point.

- On our largest lattices the ratio of the heights of the two maxima of $P_L(\beta_t, E)$ follows the prediction of the Gaussian model. The ratio of the ordered to the disordered partition function is equal to q . The finite volume corrections to the locations of the maxima of the energy follow a $1/L^d$ behavior with a slope as predicted by the large q expansion.

- The Gaussian width of the peaks of $P_L(\beta_t, E)$ approaches for large volumes the prediction of the Gaussian model with specific heat parameters C_o and C_d , which in the case of the $q=20$ Potts model are very well consistent with the large q expansion and a determination using finite size scaling. In the $q = 10$ case lattices much larger than 100^2 would be required in order to see the asymptotic behavior.

- The finite volume interface free energy estimators allow in both cases a natural extrapolation of the data to the recently calculated exact infinite volume values. Our results are consistent with those values.

- Around E_L^{min} we observe the unfolding of a flat region in $P_L(\beta_t, E)$. It is an interesting recent observation that this effect can be enhanced by using lattices which are elongated in one direction [22].

Acknowledgements: This research was partially supported by the U.S. Department of Energy under Contracts DE-FG05-87ER40319 and DE-FC05-85ER2500. We acknowledge conversations with André Morel.

References

- [1] H.J. Herrmann, W. Janke and F. Karsch (editors), *Dynamics of First Order Phase Transitions*, World Scientific, Singapore 1992.

- [2] R. B. Potts, Proc. Cambridge Philos. Soc. **48** (1952) 106;
F. Y. Wu, Rev. Mod. Phys. **54** (1982) 235.
- [3] C. Borgs and R. Kotecký, J. Stat. Phys. **61** (1990) 79.
- [4] C. Borgs, R. Kotecký and S. Miracle-Sole, J. Stat. Phys. **62** (1991) 529.
- [5] A. Billoire, T. Neuhaus and B.A. Berg, Nucl. Phys. B396 (1993) 779.
- [6] A. Klümper, Int. Journal of Mod. Phys. B4 (1990) 871;
A. Klümper, A. Schadschneider and J. Zittartz, Z. Phys. B76 (1989) 247.
- [7] E. Buffenoir and S. Wallon, Saclay preprint SPhT-92/077 (1992), to be published in Journal of Physics A..
- [8] S. Gupta, private communication;
C. Borgs and W. Janke, J. Phys. I (France) 2 (1992) 2011.
- [9] B.A. Berg and T. Neuhaus, Phys. Rev. Lett. 68 (1992) 9.
- [10] W. Janke, B.A. Berg and M. Katoot, Nucl. Phys. B382 (1992) 649.
- [11] R.J. Baxter, J. Phys. C6 (1973) L445.
- [12] T. Bhattacharya, R. Lacaze and A. Morel, Europhys. Lett., to be published.
- [13] A. Billoire, R. Lacaze and A. Morel, Nucl. Phys. B370 (1992) 773.
- [14] K. Binder, M.S. Challa and D.P. Landau, Phys. Rev. B34 (1986) 1841;
A. Billoire, R. Lacaze, A. Morel, S. Gupta, A. Irbäck and B. Petersson, Phys. Rev. B42 (1990) 6743.
- [15] J. Lee and J.M. Kosterlitz, Phys. Rev. B43 (1991) 3265.
- [16] K. Binder, Phys. Rev. A25, 1699 (1982).
- [17] S.B. Schlosman, Commun. Math. Phys. 125 (1989) 81.
- [18] B.A. Berg, U. Hansmann and T. Neuhaus, Phys. Rev. B47 (1993) 497;
Z. Phys. B90 (1993) 229.
- [19] E. Brézin and J. Zinn-Justin, Nucl. Phys. B257 (1985) 867;
M.P. Gelfand and M.E. Fisher, Physica A166 (1990) 1;
J.J. Morris, J. Stat. Phys. 69 (1991) 539.
- [20] U.-J. Wiese, preprint, BUTP-92/37.

- [21] André Morel, private conversation.
- [22] B. Grossmann and M.L. Laursen, preprint, HLRZ-93-7.

q	$F_{o.d.}$	MC estimate
7	0.020792	0.0241 (10) [10]
10	0.094701	0.0978 (08) [9]
20	0.370988	—

Table 1: *The exact interface free energy for the 2-d $q=7, 10$ and 20 Potts models, together with previous MC estimates.*

L	Msweeps
50	26
60	22
70	10

Table 2: *Additional statistics on $50^2, 60^2$, and 70^2 lattices in the $q=20$ Potts models in units of million sweeps.*

L	C_o C_d	$C_d - C_o$	$E^{max,d}$ $E^{max,o}$	R_{10} Z_o/Z_d	$F(L)$
12	4.81(06) 5.77(09)	0.97(12)	-.8813(08) -1.7666(05)	10.70(10) 11.00(09)	0.1379(04)
16	5.33(04) 6.45(06)	1.09(08)	-.9012(04) -1.7399(04)	10.25(15) 9.76(13)	0.1273(04)
24	7.06(05) 7.84(06)	0.77(09)	-.9243(06) -1.7112(05)	9.98(28) 9.46(25)	0.1168(05)
34	8.64(04) 9.43(05)	0.82(06)	-.9391(02) -1.6954(02)	10.39(57) 9.88(51)	0.1098(07)
50	10.66(09) 11.14(11)	0.37(16)	-.9504(03) -1.6835(03)	10.56(74) 10.33(69)	0.1056(06)
70	12.60(14) 13.08(23)	0.48(28)	-.9568(05) -1.6760(04)	10.2 (12) 9.7 (11)	0.1022(09)
100	13.99(20) 14.71(35)	0.54(45)	-.9612(05) -1.6712(02)	9.2 (17) 9.1 (16)	0.0997(11)
∞	18.06(4) 18.51(4)	0.44763	-.96820 -1.66425	10.12 10.0	0.094701

Table 3: *Finite volume results for the $q=10$ Potts model at β_t , together with theoretical expectations in the infinite volume limit.*

L	C_o C_d	$C_d - C_o$	$E^{max,d}$ $E^{max,o}$	R_{20} Z_o/Z_d	$F(L)$
16	3.473(10) 4.215(08)	0.742(14)	-0.60079(09) -1.85270(09)	22.40(16) 20.08(13)	0.3772(02)
18	3.486(09) 4.403(12)	0.912(16)	-0.60482(13) -1.84726(10)	22.71(28) 20.41(25)	0.3762(03)
20	3.768(32) 4.556(10)	0.789(36)	-0.60796(09) -1.84307(10)	22.19(26) 20.16(23)	0.3762(03)
24	3.895(08) 4.808(08)	0.909(12)	-0.61236(07) -1.83765(06)	22.62(24) 20.61(22)	0.3759(02)
30	4.196(12) 5.109(12)	0.908(16)	-0.61653(09) -1.83265(07)	21.44(39) 19.66(36)	0.3751(03)
32	4.270(13) 5.213(14)	0.942(17)	-0.61761(09) -1.83149(07)	21.66(65) 19.85(59)	0.3758(03)
34	4.370(26) 5.204(36)	0.831(35)	-0.61856(14) -1.83048(11)	22.87(46) 20.98(36)	0.3766(10)
38	4.495(13) 5.356(18)	0.863(24)	-0.61980(08) -1.82877(06)	20.84(68) 19.24(63)	0.3747(05)
50	4.739(20) 5.603(26)	0.864(36)	-0.62236(14) -1.82572(09)	23.9 (24) 22.1 (22)	0.3747(09)
60	4.925(19) 5.693(30)	0.768(30)	-0.62334(14) -1.82410(10)	26.0 (41) 24.3 (38)	0.3738(09)
70	5.004(28) 5.825(31)	0.821(42)	-0.62430(13) -1.82334(10)	27.0 (45) 25.1 (42)	0.3732(13)
∞	5.362(3) 6.133(3)	0.77139	-0.62653 -1.82068	21.5 20.0	0.370988

Table 4: *Finite volume results for the $q=20$ Potts model at β_t , together with theoretical expectations in the infinite volume limit.*

L	E_L^+	E_L^-
50	-1.00	-1.35
60	-1.00	-1.32
70	-1.01	-1.36
bubble	-1.01	-1.44

Table 5: *Prediction of the spherical bubble model (last line) together with estimated locations on 50^2 , 60^2 and 70^2 lattices in the $q=20$ Potts model.*

fit	L_{min}	$F_{o.d.}$	$\chi^2/d.o.f$
$a_2 = a_3 = b = 0^{(*)}$	12	0.0950(05)	.218
	16	0.0949(06)	.220
	24	0.0946(08)	.206
	34	0.0949(13)	.257
	50	0.0938(20)	.003
$a_3 = b = 0$	12	0.0946(09)	.176
	16	0.0943(13)	.218
	24	0.0947(23)	.307
	34	0.0924(39)	.041
$b = 0$	12	0.0942(19)	.221
	16	0.0945(33)	.325
	24	0.0905(64)	.103
$a_2 = a_3 = 0$	12	0.0941(15)	.167
	16	0.0939(22)	.217
	24	0.0945(40)	.308
	34	0.0903(69)	.062
Theory		0.094701	

Table 6: Results of fits of the form eq.(16) to the finite volume estimators $F(L)$ of Table 3 for the $q=10$ Potts model. Column one specifies which parameters of the fit were fixed to 0, with $b = -p + d/2$. The fit intervals are from L_{min} of column two to $L_{max} = 100$. The fit marked with $(*)$ denotes the fit which results into our infinite volume estimate eq.(18). It has been plotted in figure 10.

fit	L_{min}	$F_{o.d.}$	$\chi^2/d.o.f$	consistent with theory
$a_2 = a_3 = b = 0$ (*)	16	0.3736(04)	1.187	no
	18	0.3739(05)	1.184	no
	20	0.3736(06)	1.179	no
	24	0.3733(07)	1.306	no
	30	0.3726(12)	1.470	no
	32	0.3714(13)	.590	yes
	34	0.3713(17)	.782	yes
	38	0.3724(19)	.265	yes
	50	0.3694(45)	.001	yes
$a_3 = b = 0$	16	0.3733(12)	1.330	no
	18	0.3717(15)	.985	yes
	20	0.3716(17)	1.149	yes
	24	0.3709(23)	1.329	yes
	30	0.3663(46)	1.335	no
	32	0.3726(59)	.773	yes
	34	0.3766(94)	1.009	yes
	38	0.362 (13)	.028	yes
$b = 0(**)$	16	0.3684(29)	1.033	yes
	18	0.3701(38)	1.116	yes
	20	0.3687(46)	1.287	yes
	24	0.363 (10)	1.528	yes
	30	0.390 (21)	1.368	yes
	32	0.358 (31)	1.057	yes
$a_2 = a_3 = 0$	16	0.3727(20)	1.312	yes
	18	0.3698(25)	.962	yes
	20	0.3699(30)	1.121	yes
	24	0.3688(40)	1.312	yes
	30	0.3608(88)	1.383	no
	32	0.373 (11)	.777	yes
	34	0.379 (18)	1.064	yes
	38	0.354 (25)	.037	yes
Theory		0.370988		

Table 7: Results of fits of the form eq.(16) to the finite volume estimators $F(L)$ of Table 4 for the $q=20$ Potts model. Column one specifies which parameters of the fit where fixed to 0, with $b = -p + d/2$. The fit intervals are from L_{min} of column two to $L_{max} = 70$. The last column specifies whether the exact $F_{o.d.}$ result is within one standard deviation of the fitted value. The fit marked with (*) denotes the fit which results into our infinite volume estimate eq.(19), the one marked with (**) has been plotted in figure 11.

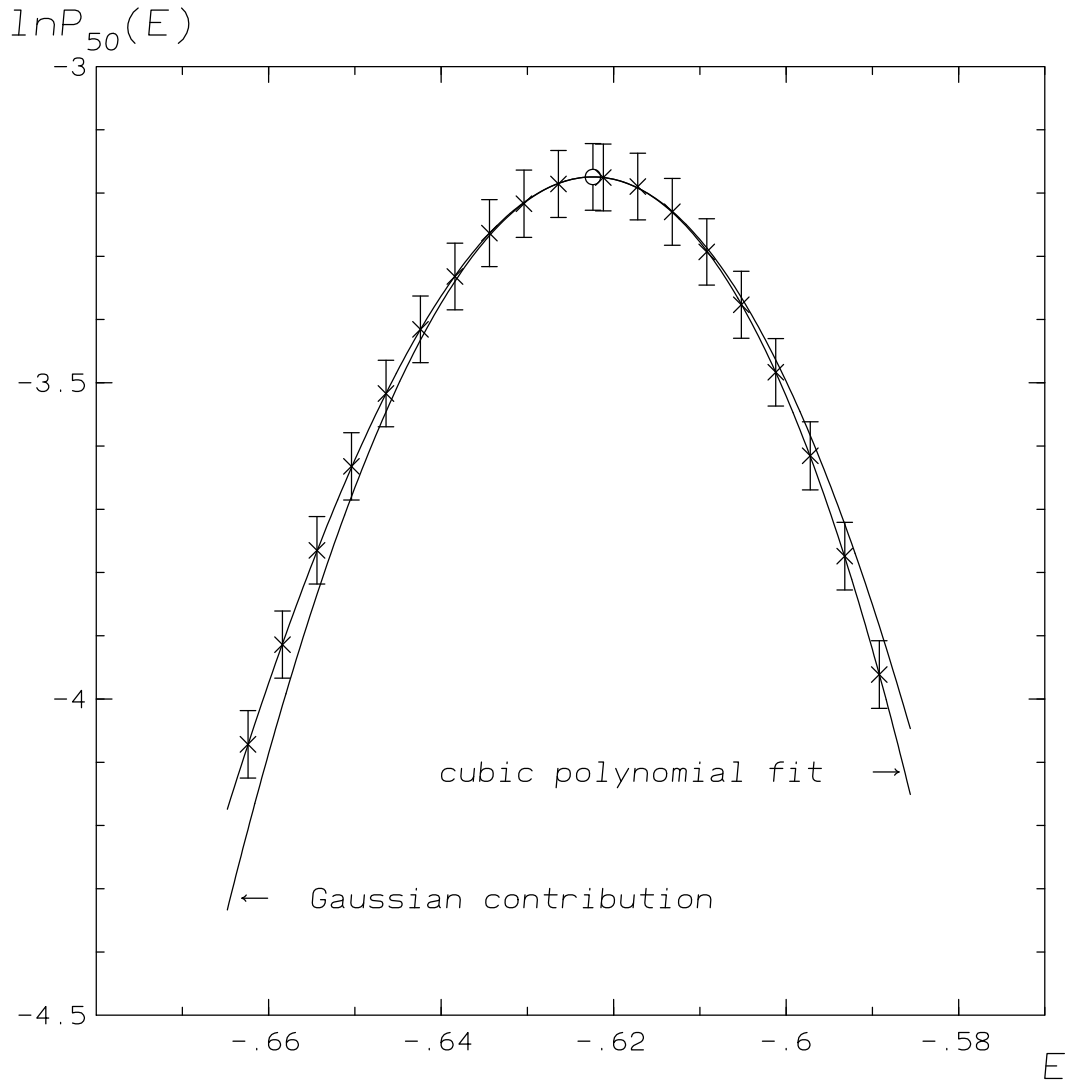


FIG. 1

Figure 1: Plot of $\ln P_L(\beta_t, E)$ on a 50^2 lattice for the $q=20$ Potts model in the vicinity of the disordered state. The crosses denote (selected) data with their error bars. The circle denotes the maximum value $P_L^{max,d}$ with error bar. The two curves display a cubic polynomial fit to $\ln P_L(\beta_t, E)$ and the Gaussian contribution to this fit.

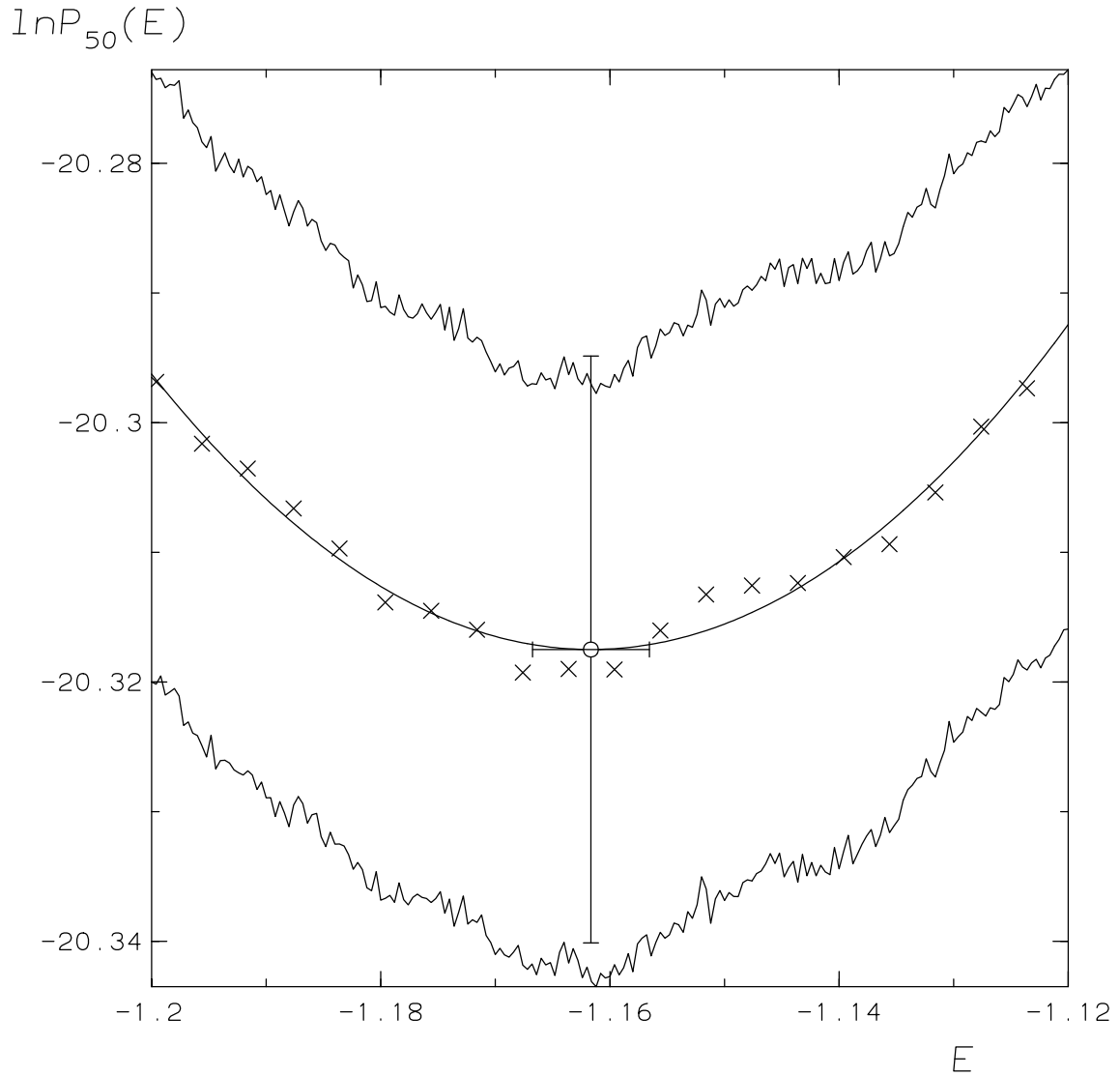


FIG. 2

Figure 2: Plot of $\ln P_L(\beta_t, E)$ on a 50^2 lattice in the $q=20$ Potts model in vicinity of P_L^{min} . The crosses denote selected data. The wiggling curves indicate the error interval of the data, while the circle with error bars denotes our estimate of P_L^{min} and E_L^{min} .

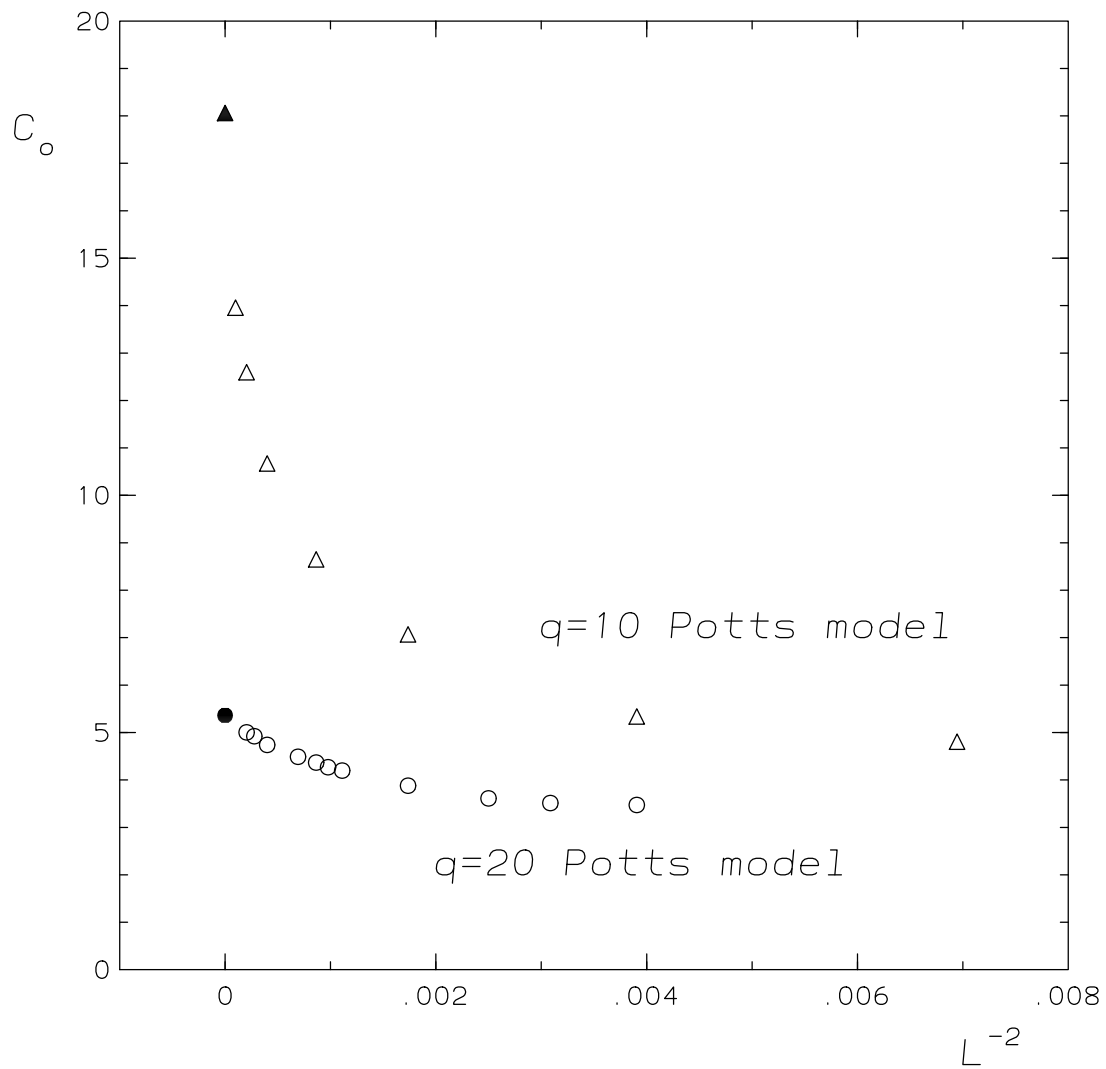


FIG. 3

Figure 3: Estimates of C_o for the $q=10$ (circles) and $q=20$ Potts (triangles) models, as extracted from the width of the ordered peak of $P_L(\beta_t, E)$. The full symbols denote asymptotic results from the large q -expansion.

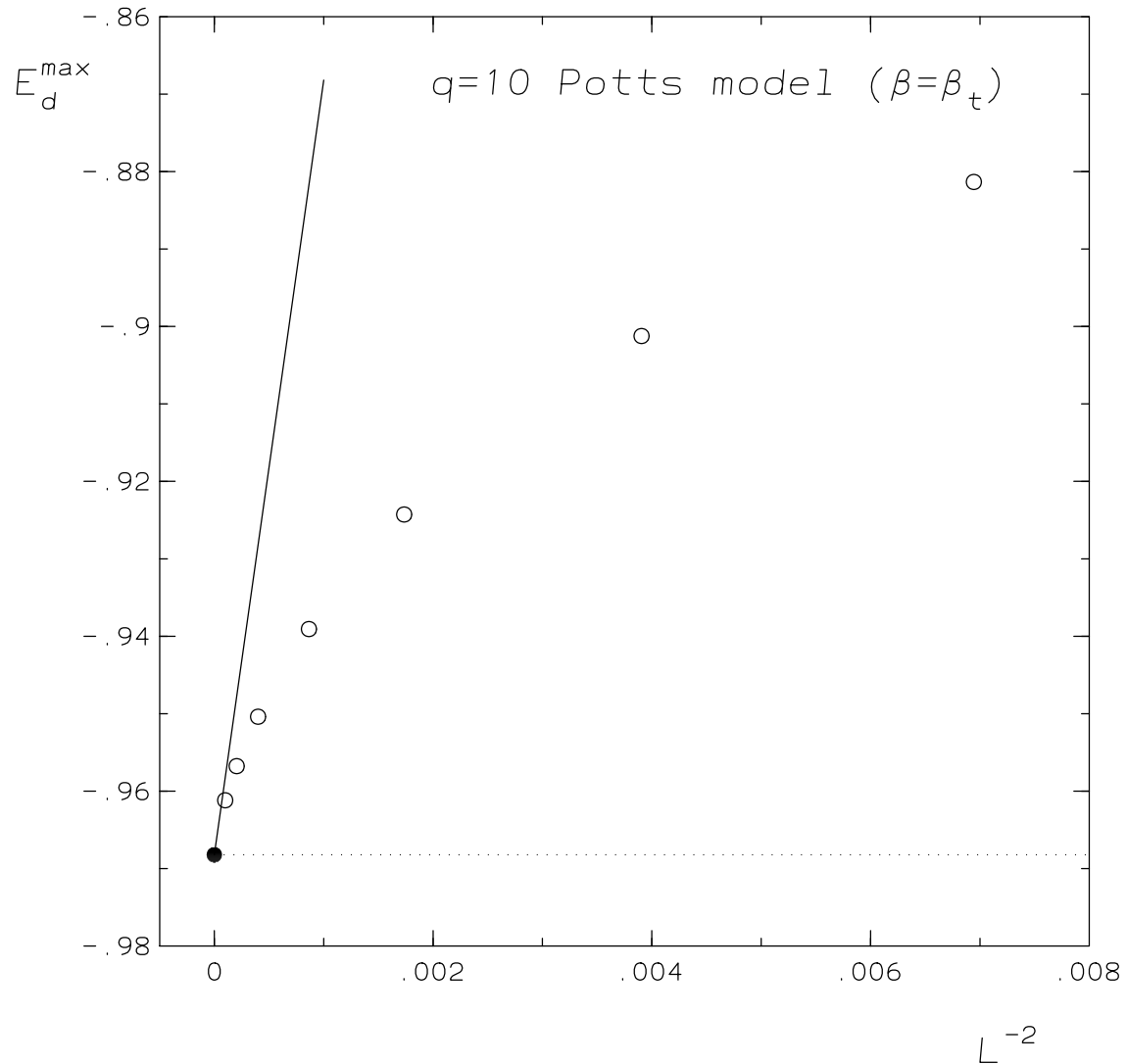


FIG. 4

Figure 4: Locations of the maxima of disorder states $E_L^{max,d}$ at β_t in the $q=10$ Potts model as function of the inverse volume. The full symbol and dashed line denote the infinite volume prediction. The full line has a slope $g'''/(2g'')$ as predicted by the large q expansion [12].

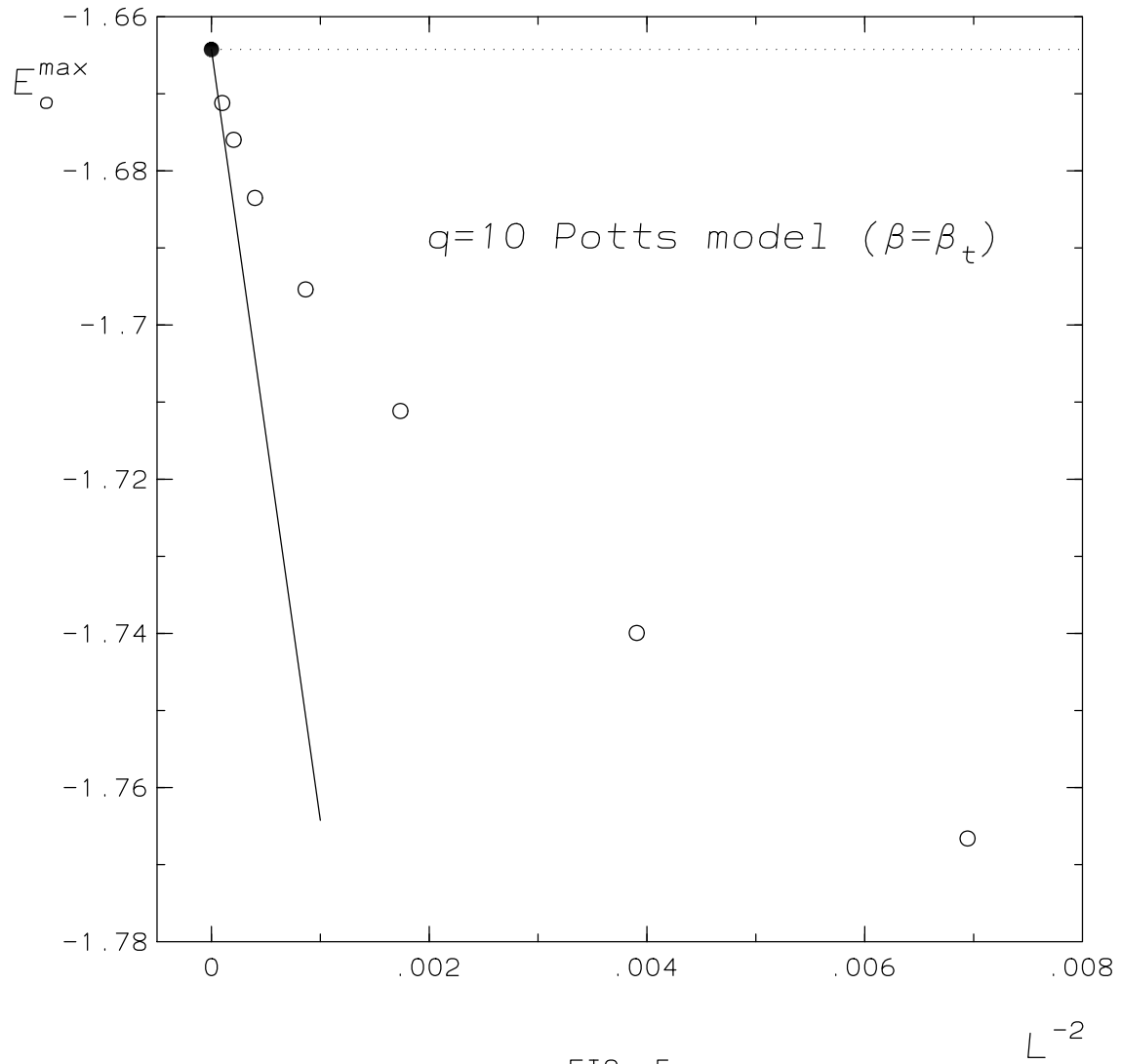


FIG. 5

Figure 5: Locations of the maxima of ordered states $E_L^{max,o}$ at β_t in the $q=10$ Potts model as function of the inverse volume. The symbols and lines have the same meaning as in Fig. 4.

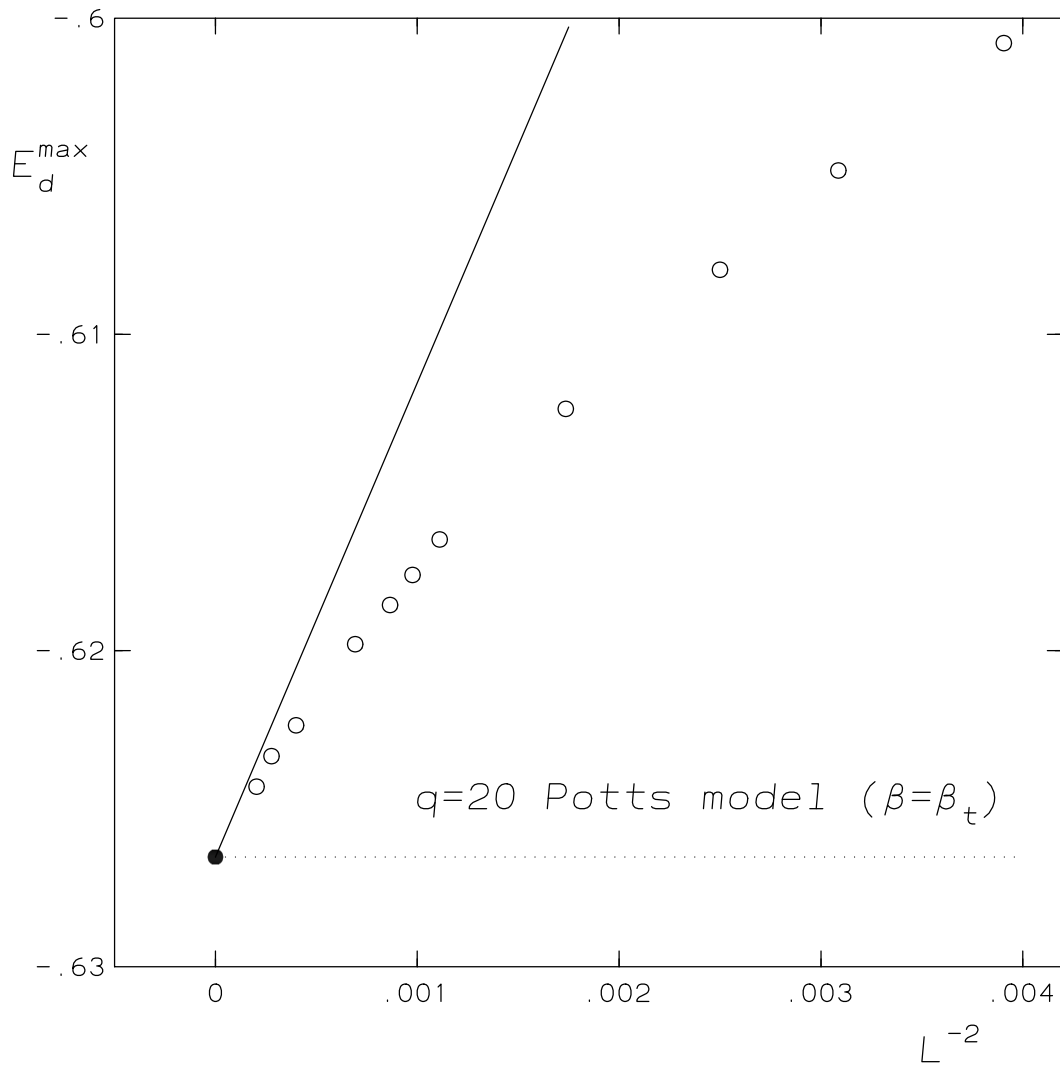


FIG. 6

Figure 6: Locations of the maxima of disordered states $E_L^{\max,d}$ at β_t in the $q=20$ Potts model as function of the inverse volume. The symbols and lines have the same meaning as in Fig. 4.

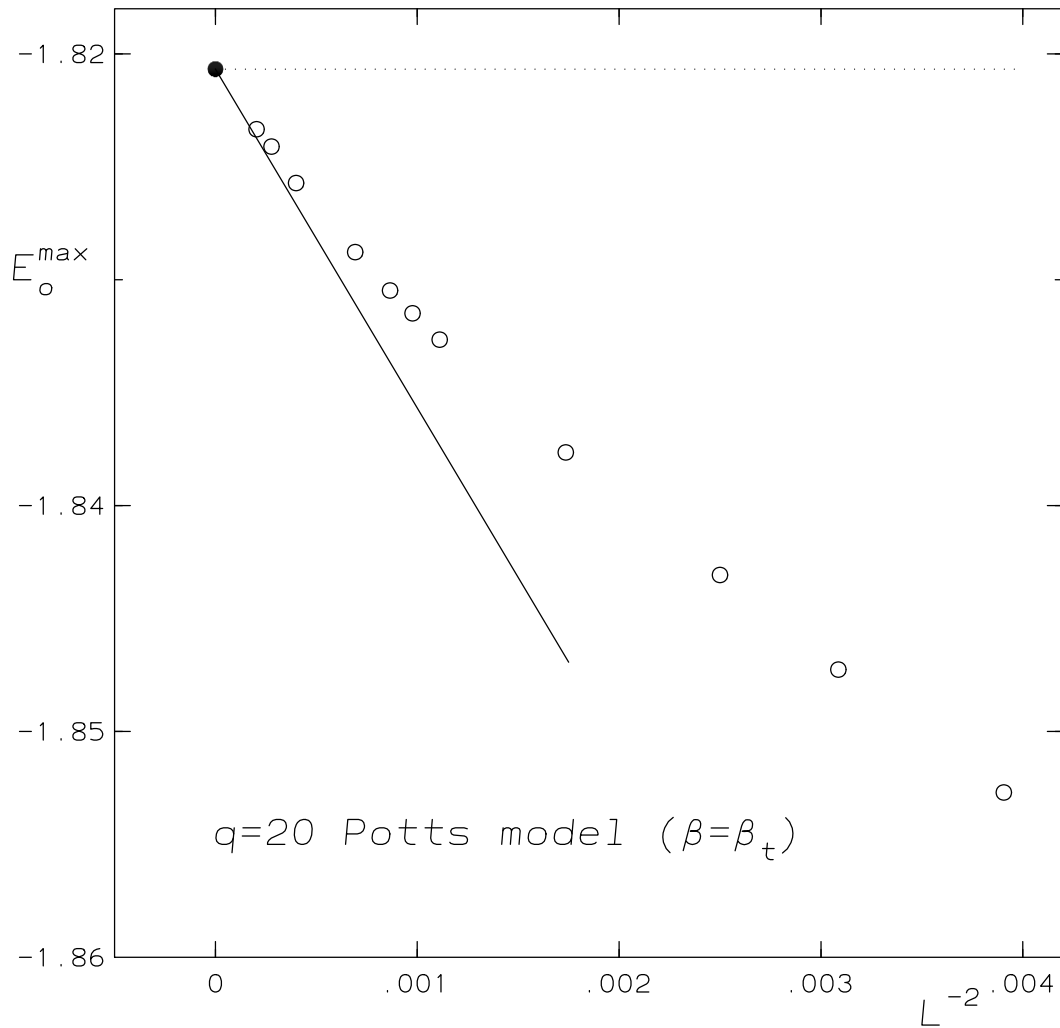


FIG. 7

Figure 7: Locations of the maxima of ordered states $E_L^{max,o}$ at β_t in the $q=20$ Potts model as function of the inverse volume. The symbols and lines have the same meaning as in Fig. 4.

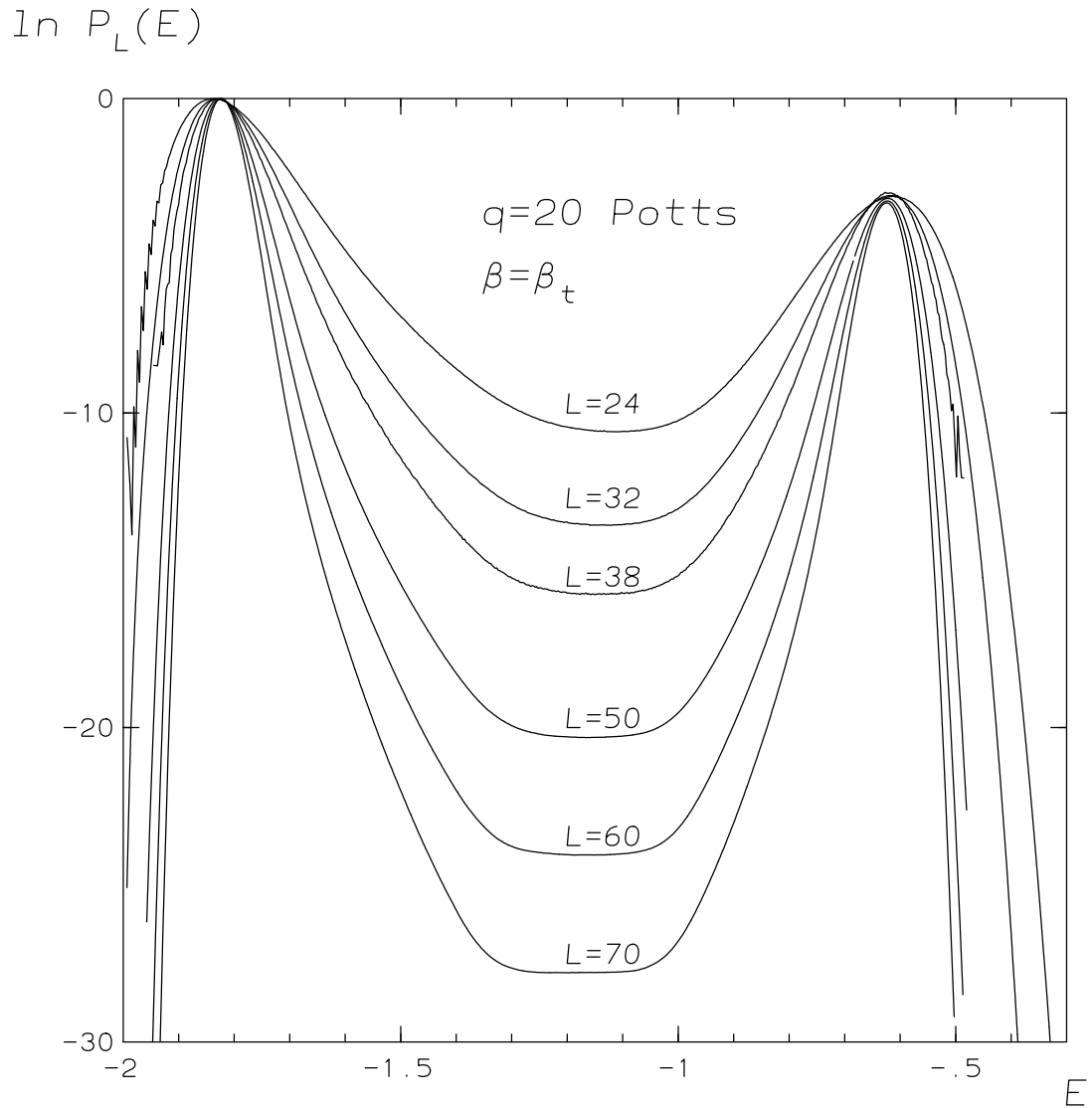


FIG. 8

Figure 8: Plot of $\ln P_L(\beta_t, E)$ for selected lattice sizes in the $q=20$ Potts model. The unfolding of a flat region with increasing lattice size $L > 38$ is observed.

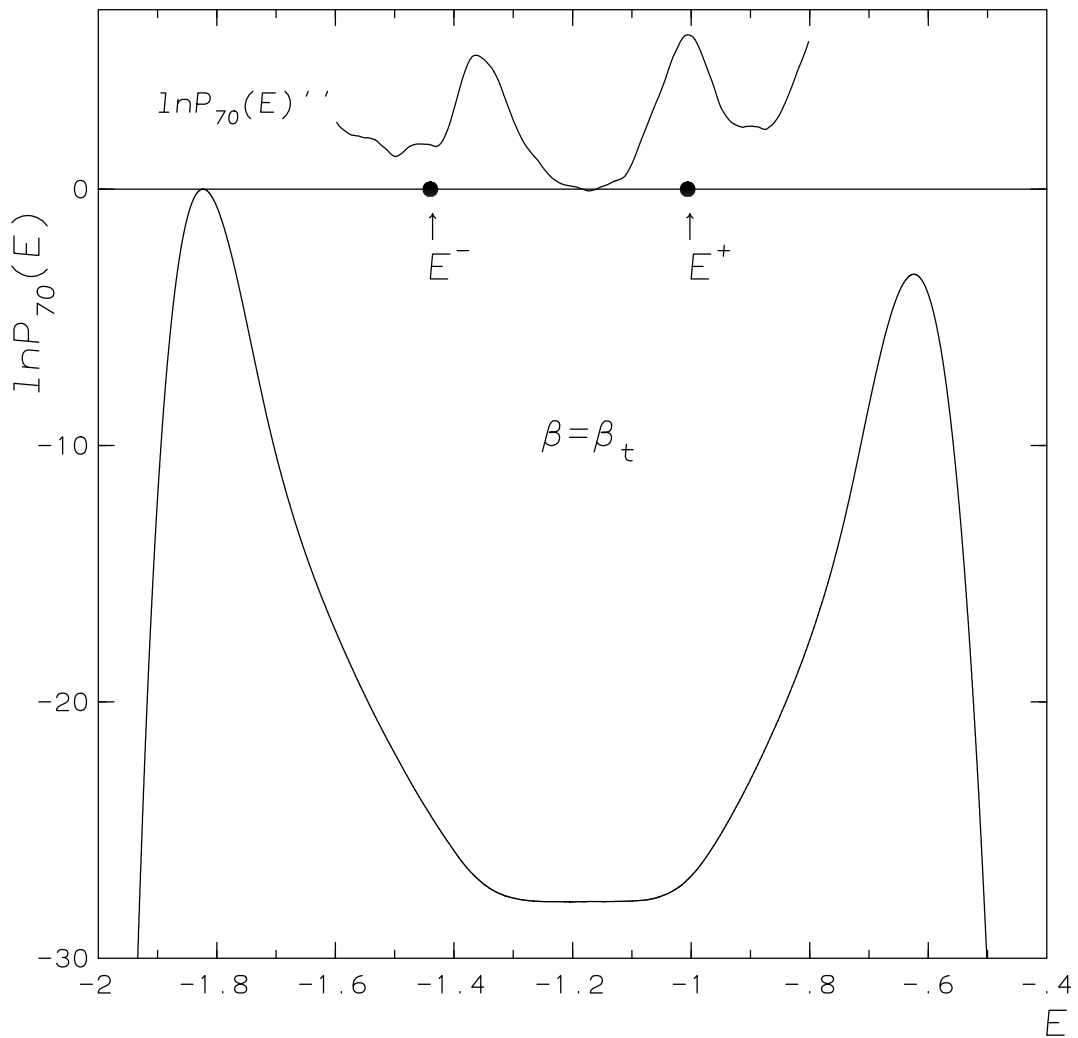


FIG. 9

Figure 9: Plot of $\ln P_L(\beta_t, E)$ on a 70^2 lattice. The statistical errors cannot be resolved. In the upper half of the plot we display a numerical estimate of the curvature of $\ln P_L(\beta_t, E)$. The transition from the two planar interface to the single bubble region is indicated by two peaks. Their position is compared with the prediction for spherical bubbles .

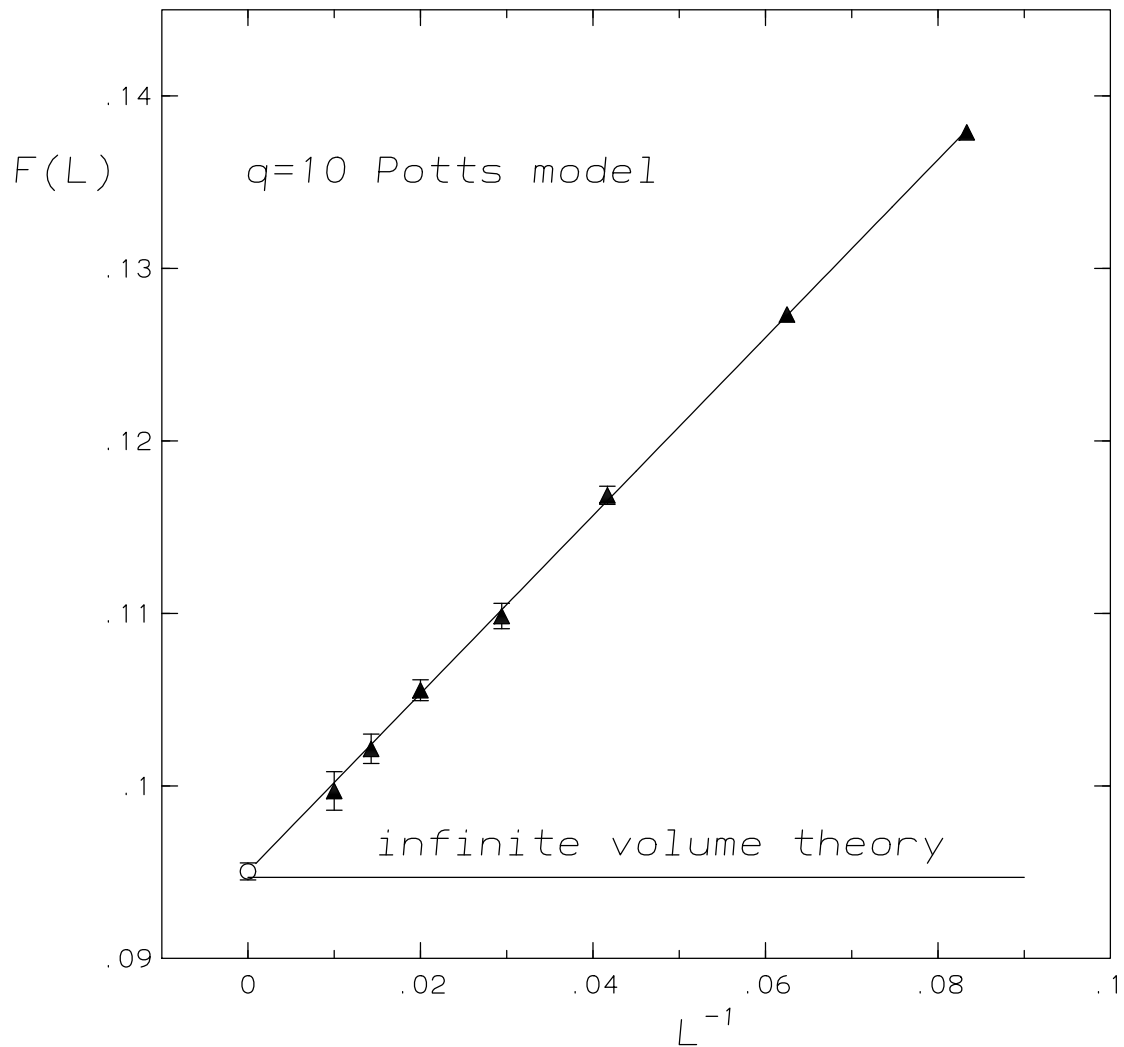


FIG. 10

Figure 10: Plot of the finite volume estimator $F(L)$ for the $q=10$ Potts model as function of $1/L$. The horizontal line corresponds to the theoretical value, and a fit of the form $F(L) = F_{o.d.} + a_1/L$ is displayed.

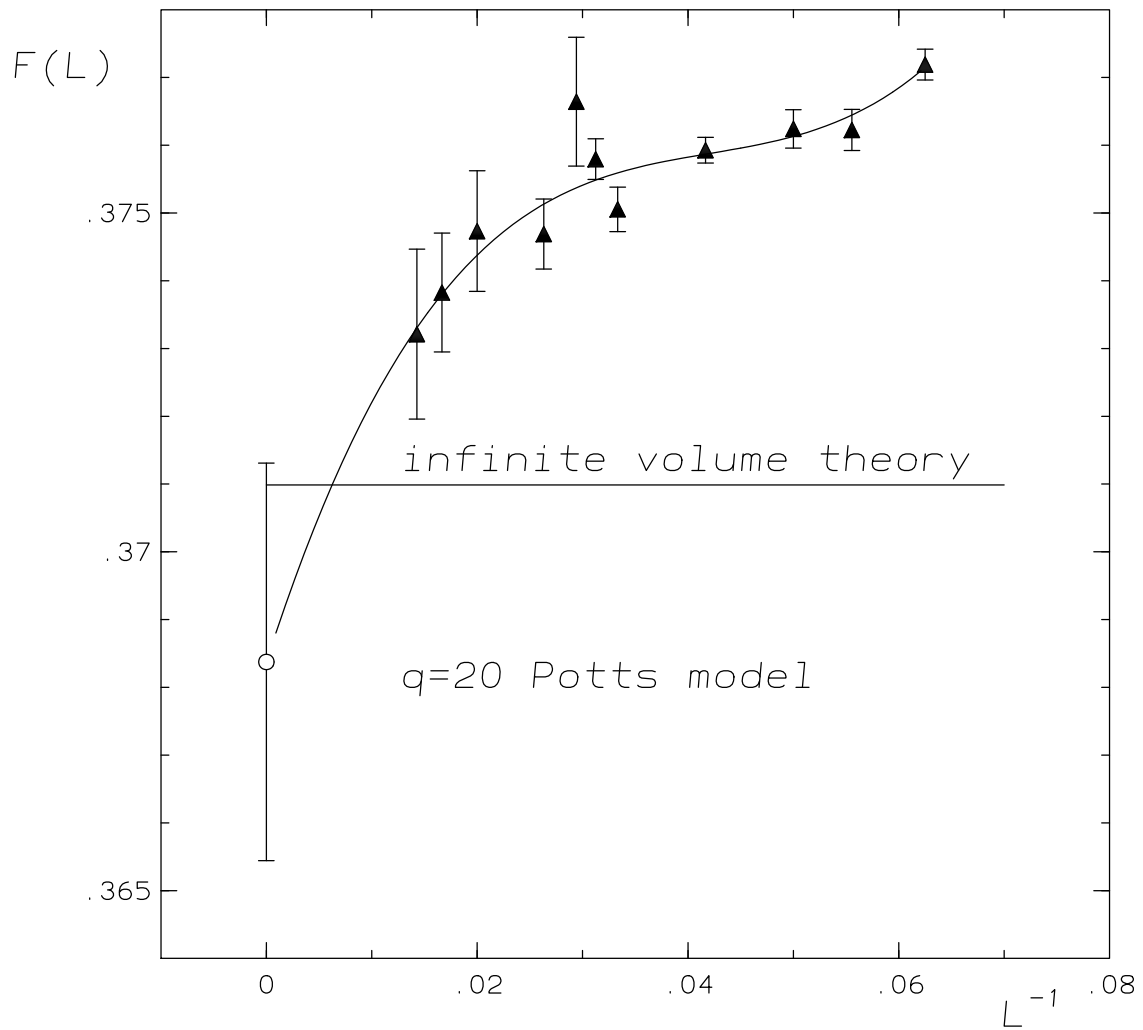


FIG. 11

Figure 11: Plot of the finite volume estimator $F(L)$ for the $q=20$ Potts model as function of $1/L$. The horizontal line corresponds to the theoretical value, and a fit of the form $F(L) = F_{o.d.} + a_1/L + a_2/L^2 + a_3/L^3$ is displayed.